

Modelling and simulation of the delamination in composite materials

C A Vieira Carneiro and M A Savi*

Department of Mechanical and Materials Engineering, Instituto Militar de Engenharia, Rio de Janeiro, Brazil

Abstract: Delamination is a phenomenon characterized by the loss of adhesion between two adjacent laminae. This is a damage process frequently observed in composite materials and it may cause either loss of structural stiffness or total failure of the laminate. This contribution presents a model to describe composite delamination. The proposed model considers a laminate with a finite thickness interlayer. Interlaminar stresses are evaluated from a modified lamination theory. This result is used as input in the constitutive adhesion model which describes the damage evolution of the interlayer. An iterative numerical procedure is developed, solving the model equations separately. This work considers numerical simulations of a laminated tube and a laminated bar as applications of the proposed general formulation. Numerical results are capable of capturing the general behaviour of experimental data.

Keywords: composite materials, delamination, constitutive equations

NOTATION

a, b, c, k	interface constitutive constants	W	set associated with the thermodynamic force Y
A_{mnr}, B_{mnr}	tensors related to the elastic tensor	x_1, x_2, x_3	coordinate axes
C	set associated with the damage variable	X^R, Y	thermodynamic forces
C_1, C_2	constants related to the solution of the laminated tube	γ	damage variable
D_1, D_2	constants related to the solution of the laminated tube	δ	thickness of the interface
D_1^v, K_1^v	constants related to the solution of the laminated bar	$\Delta u, \Delta v$	displacement differences
E_1, E_2	elastic moduli	$\Delta \sigma_{ij}$	constraint stress tensor
G	shear modulus of the interlayer	$\varepsilon_{mn}^l, \varepsilon_{mn}^u$	strain tensors of the lower and upper laminae respectively
G_{12}^l, G_{12}^u	shear moduli of the lower and upper laminae respectively	$\varepsilon_{mn}^{u/l}$	interlaminar strain tensor
h	thickness of the lamina	$\varepsilon_{13}, \varepsilon_{23}$	interlaminar deformations
$I_{(\cdot)}$	indicator function associated with the set (\cdot)	θ	angle which defines the orientation of the fibres
l	length of the half-bar or tube	ν_{12}	Poisson's ratio
r	relative displacement between two points of the interlayer	ρ	specific mass
s	entropy	σ_{ij}	stress tensor
S_{klpq}^l, S_{klpq}^u	compliance tensors of the lower and upper laminae respectively	τ_{13}, τ_{23}	interlaminar stresses
T_{ijkl}^l, T_{ijkl}^u	transformation tensors of the lower and upper laminae respectively	ϕ^*	dual of the dissipation potential
		ψ	Helmholtz free energy
		$\partial_{(\cdot)}$	subdifferential with respect to the variable (\cdot)

1 INTRODUCTION

The basic building block of a composite material is the lamina, which usually consists of a reinforced fibre matrix. Several laminae are usually bonded together to act as an integral structural element denoted as a laminate. The degradation modes of composite laminates can be split into

The MS was received on 23 August 1999 and was accepted after revision for publication on 28 April 2000.

*Corresponding author: Department of Mechanical and Materials Engineering, Instituto Militar de Engenharia, 22.290.270 Rio de Janeiro, Brasil.

two classes: intralaminar damage and delamination. Intralaminar damage includes transverse matrix cracking, fibre–matrix debonding and fibre ruptures. On the other hand, delamination is a phenomenon characterized by the loss of adhesion between two adjacent laminae. This is a damage process frequently observed in composite materials and it may cause either loss of structural stiffness or total failure of the laminate. Delamination may be caused by interlaminar stress concentration, which occurs either in the neighbourhood of the free edge or around loaded holes of the composite [1].

The study of delamination process may be carried out by two different approaches. The first is fracture mechanics, which considers the failure modes of the material. This approach is most disseminated and much research has been developed in this field [2–7]. The second approach considers phenomenological constitutive equations to describe the interlaminar behaviour. Usually, the interlayer is considered as a surface, neglecting its thickness. Therefore, delamination is characterized by the loss of contact between the laminae [1, 8–14].

This contribution presents a model to describe composite delamination. The proposed model considers a laminate with a finite thickness interlayer. Interlaminar stresses are evaluated from a modified lamination theory proposed by Bai *et al.* [15]. This result is used as input in a constitutive adhesion model which describes the damage evolution of the interlayer. The constitutive model is formulated within the formalism of continuum mechanics and thermodynamics of irreversible processes and is based on the adhesion model proposed in references [1], [9], [10] and [12]. An iterative numerical procedure is developed, solving the model equations separately. Finally, this work considers numerical simulations of a laminated tube and a laminated bar as applications of the proposed general formulation. Numerical results show that the model is capable of capturing the general behaviour of experimental data.

2 MODIFICATION OF CLASSICAL LAMINATION THEORY

The determination of interlaminar stresses is very important to analyse delamination phenomena. The classical lamination theory has a serious limitation to predict this kind of stress because it conceives just in-plane stresses, neglecting the others, which can cause delamination [3]. Therefore, the determination of the interlaminar stresses must consider a three-dimensional approach. Pipes and Pagano [16] proposes a three-dimensional elasticity solution to analyse a laminate under uniaxial extension using a finite difference scheme. The finite element analysis has also been employed by many researchers to investigate this problem [2, 3, 17–21]. This contribution evaluates the interlaminar stresses by considering a modification of classical lamination theory proposed by Bai *et al.* [15]. With this aim, a two-layer laminated element, each with thickness h and an interlayer with finite thickness δ , as depicted in Fig. 1, is considered.

Interlaminar deformations ε_{13} and ε_{23} result from the interlaminar stresses τ_{13} and τ_{23} induced by the stiffness mismatch between laminae. Since the interlaminar deformation in each lamina is much smaller than at each interface due to imperfect interfacial bonding, it is assumed that there is no interlaminar deformation in each lamina and all interlaminar deformation occurs in the interlayer. Therefore, the two-layer laminate with rectangular coordinates (x_1, x_2, x_3) , where the x_1x_2 plane coincides with the mid-plane of the laminate, is considered. The in-plane stresses on each lamina consist of the sum of the stress σ_{ij} ($i, j = 1, 2$) due to external loads and the constraint stress $\Delta\sigma_{ij}$ ($i, j = 1, 2$) provided by its adjacent laminae:

$$\sigma_{ij}^u = \sigma_{ij} + \Delta\sigma_{ij} \quad (1a)$$

$$\sigma_{ij}^l = \sigma_{ij} - \Delta\sigma_{ij} \quad (1b)$$

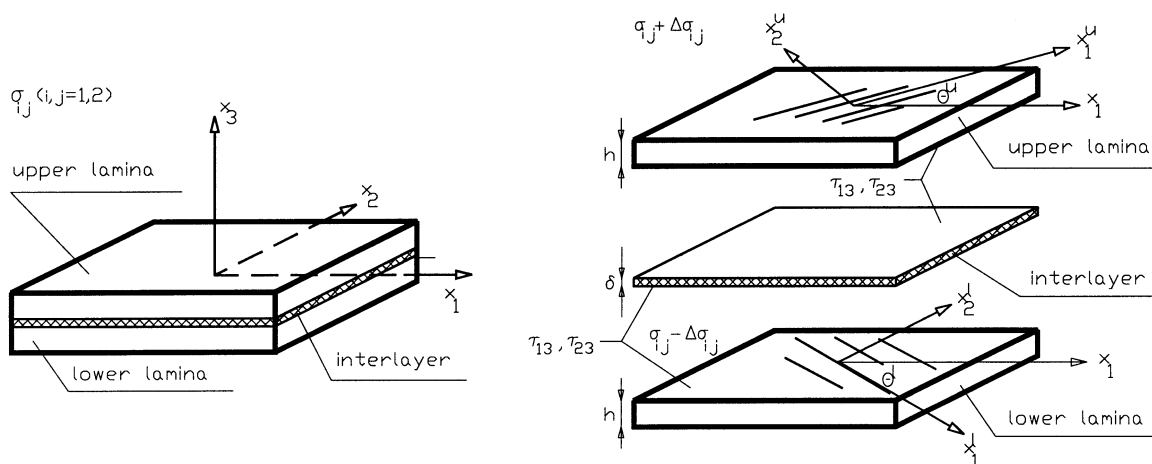


Fig. 1 Laminate with interlayer

where the superscripts u and l are associated with the upper and lower laminae respectively.

By considering the compliance tensors S_{ijkl}^u and S_{ijkl}^l of the laminae, it is possible to write the stress-strain relations on each lamina:

$$\epsilon_{ij}^u = S_{ijkl}^u \sigma_{kl}^u \quad (2a)$$

$$\epsilon_{ij}^l = S_{ijkl}^l \sigma_{kl}^l \quad (2b)$$

Now, taking into account the stress transformation tensors T_{ijkl}^u and T_{ijkl}^l , the strains on each lamina are obtained [15]:

$$\epsilon_{mn}^u = T_{mnl}^u S_{klpq}^u T_{pqrs}^u (\sigma_{rs} + \Delta\sigma_{rs}) \quad (3a)$$

$$\epsilon_{mn}^l = T_{mnl}^l S_{klpq}^l T_{pqrs}^l (\sigma_{rs} - \Delta\sigma_{rs}) \quad (3b)$$

At this point, the interlaminar strains are evaluated as follows:

$$2\epsilon_{mn}^{u/l} = \epsilon_{mn}^u - \epsilon_{mn}^l = B_{mnr} \Delta\sigma_{rs} + A_{mnr} \sigma_{rs} \quad (4)$$

where

$$B_{mnr} = T_{mnl}^u S_{klpq}^u T_{pqrs}^u + T_{mnl}^l S_{klpq}^l T_{pqrs}^l \quad (5a)$$

$$A_{mnr} = T_{mnl}^u S_{klpq}^u T_{pqrs}^u - T_{mnl}^l S_{klpq}^l T_{pqrs}^l \quad (5b)$$

According to the linear shear slip theory [22], the differences between the displacements of the upper and the lower surfaces of the interlayer are given by

$$\Delta u(x_1, x_2, x_3) = \frac{\delta}{G} \tau_{13}(x_1, x_2) \quad (6a)$$

$$\Delta v(x_1, x_2, x_3) = \frac{\delta}{G} \tau_{23}(x_1, x_2) \quad (6b)$$

where Δu and Δv are the displacement differences in the x_1 and x_2 directions respectively. The constant G is the shear modulus of the interlayer.

For continuity conditions, the in-plane displacements of the upper and the lower laminae must be equal to the displacements of the upper and lower surfaces of the interlayer. Therefore, assuming infinitesimal strain hypothesis and linear elastic relations, it is possible to write

$$\epsilon_{11}^{u/l} = \frac{\delta}{2G} \frac{\partial \tau_{13}}{\partial x_1} \quad (7a)$$

$$\epsilon_{22}^{u/l} = \frac{\delta}{2G} \frac{\partial \tau_{23}}{\partial x_2} \quad (7b)$$

$$\epsilon_{12}^{u/l} = \frac{\delta}{4G} \left(\frac{\partial \tau_{23}}{\partial x_1} + \frac{\partial \tau_{13}}{\partial x_2} \right) \quad (7c)$$

Establishing the equilibrium on the lamina element [15], the following equations are obtained:

$$\left[\frac{\partial(\Delta\sigma_{11})}{\partial x_1} + \frac{\partial(\Delta\sigma_{12})}{\partial x_2} \right] h - \tau_{13} = 0 \quad (8a)$$

$$\left[\frac{\partial(\Delta\sigma_{22})}{\partial x_2} + \frac{\partial(\Delta\sigma_{12})}{\partial x_1} \right] h - \tau_{23} = 0 \quad (8b)$$

Using these results in the equations of interlaminar strain [equation (7)] and then, in equation (4), the constraint stresses $\Delta\sigma_{11}$, $\Delta\sigma_{22}$ and $\Delta\sigma_{12}$ can be obtained from the following set of differential equations:

$$\begin{aligned} & (B_{1111} \Delta\sigma_{11} + B_{1122} \Delta\sigma_{22} + B_{1112} \Delta\sigma_{12}) \\ & - \frac{\delta}{G} \left[\frac{\partial^2(\Delta\sigma_{11})}{\partial x_1^2} + \frac{\partial^2(\Delta\sigma_{12})}{\partial x_1 \partial x_2} \right] h \\ & = -(A_{1111} \sigma_{11} + A_{1122} \sigma_{22} + A_{1112} \sigma_{12}) \end{aligned} \quad (9)$$

$$\begin{aligned} & (B_{2211} \Delta\sigma_{11} + B_{2222} \Delta\sigma_{22} + B_{2212} \Delta\sigma_{12}) \\ & - \frac{\delta}{G} \left[\frac{\partial^2(\Delta\sigma_{22})}{\partial x_2^2} + \frac{\partial^2(\Delta\sigma_{12})}{\partial x_1 \partial x_2} \right] h \\ & = -(A_{2211} \sigma_{11} + A_{2222} \sigma_{22} + A_{2212} \sigma_{12}) \end{aligned} \quad (10)$$

$$\begin{aligned} & (B_{1211} \Delta\sigma_{11} + B_{1222} \Delta\sigma_{22} + B_{1212} \Delta\sigma_{12}) \\ & - \frac{\delta}{2G} \left[\frac{\partial^2(\Delta\sigma_{11})}{\partial x_1 \partial x_2} + \frac{\partial^2(\Delta\sigma_{22})}{\partial x_1 \partial x_2} + \frac{\partial^2(\Delta\sigma_{12})}{\partial x_1^2} + \frac{\partial^2(\Delta\sigma_{12})}{\partial x_2^2} \right] h \\ & = -(A_{1211} \sigma_{11} + A_{1222} \sigma_{22} + A_{1212} \sigma_{12}) \end{aligned} \quad (11)$$

3 ADHESION MODEL

The thermodynamic state of a solid is completely defined by the knowledge of state variables. Constitutive equations may be formulated within the formalism of continuum mechanics and thermodynamics of irreversible processes, by considering thermodynamic forces, defined from the Helmholtz free energy ψ , and thermodynamic fluxes, defined from the dissipation pseudo-potential ϕ [23]. The adhesion model here proposed is based on the constitutive model proposed in references [1] and [9] to [12].

With this aim, consider a variable associated with the relative displacement between two points of the interlayer,

with the same coordinates (x_1, x_2) , r . In this article, the following definition is considered:

$$r = \sqrt{\Delta u^2 + \Delta v^2} \quad (12)$$

In order to evaluate adhesion, a damage variable γ is introduced. This variable is associated with bonded surfaces and assumes the following values: $\gamma = 0$, when there is total adhesion; $0 < \gamma < 1$, when the adhesion is partial; $\gamma = 1$, when there is no adhesion. In fact, this variable represents two kinds of damage associated with the adhesive damage between upper and lower laminae and the interlayer. The damage associated with intralaminar behaviour is not included in this model.

After these considerations, the interlayer state may be defined by the pair (r, γ) , which represents the state variables of the delamination phenomenon. At this point, consider a Helmholtz free energy with the form

$$\psi(r, \gamma) = \frac{k}{2}(1 - \gamma)^2 r^2 + \frac{a}{2} r^2 + I_C(\gamma) \quad (13)$$

where k and a are constants; I_C represents the indicator function associated with the set C defined as follows [24]:

$$C = \{\gamma: 0 \leq \gamma \leq 1, \dot{\gamma} \geq 0\} \quad (14)$$

The thermodynamic forces are given by [23]

$$X^R \in \partial_r \psi(r, \gamma) = [k(1 - \gamma)^2 + a]r \quad (15)$$

$$Y \in -\partial_\gamma \psi(r, \gamma) = k(1 - \gamma)r^2 - \partial_\gamma I_C \quad (16)$$

where $\partial_i \psi$ is the subdifferential of the Helmholtz free energy with respect to the variable i [24].

Now, consider the dual of the dissipation potential:

$$\phi^*(X^R, Y) = \frac{b}{2} Y^2 + \frac{c}{2} (X^R)^2 + I_W(Y) \quad (17)$$

where b and c are constants; I_W represents the indicator function associated with the set W defined as follows:

$$W = \{Y: Y \geq 0\} \quad (18)$$

The evolution equations of state variables are given by the following definitions [23]:

$$\dot{r} \in \partial_{X^R} \phi^*(X^R, Y) = cX^R \quad (19)$$

$$\dot{\gamma} \in \partial_Y \phi^*(X^R, Y) = bY + \partial_Y I_W \quad (20)$$

where $\partial_i \phi^*$ is the subdifferential of the dual of the dissipation potential with respect to a thermodynamic force

i . Since the dissipation pseudo-potential, or its dual, is convex positive and vanishes at the origin [24], the Clausius–Duhem inequality [25]

$$\sigma: \dot{\epsilon} - \rho(\dot{\psi} + s\dot{T}) \geq 0 \quad (21)$$

is automatically satisfied if the entropy is defined as $s = -\partial\psi/\partial T$ [23].

4 NUMERICAL PROCEDURE

The numerical procedure here proposed has two parts. In the first, interlaminar stresses are evaluated using the modification of the classical lamination theory proposed by Bai *et al.* [15]. The next step of solution consists in evaluating the evolution of the state variables of the adhesion model. An iterative procedure assures the convergence of the procedure.

The determination of interlaminar stresses may be either analytical or numerical, solving equations (9) to (11). From this solution, it is possible to calculate relative displacements, which are used as input in the adhesion model. Time discretization is necessary to evaluate the evolution of state variables. By considering the implicit Euler algorithm, the following equations are written:

$$(X^R)_n^i = [k(1 - \gamma_n^i)^2 + a]r_n^i \quad (22)$$

$$Y_n^i = k(1 - \gamma_n^i)(r_n^i)^2 - \partial_\gamma I_C \quad (23)$$

$$\gamma_n^i = \gamma_{n-1}^i + \Delta t(bY_n^i + \partial_Y I_W) \quad (24)$$

where the superscript i is associated with space, while the subscript n is associated with the time instant. The subdifferential $\partial_\gamma I_C$ is numerically treated by considering the projection of the variable γ on the set C , while $\partial_Y I_W$ considers the projection of Y on the set W .

An iterative numerical procedure is employed until some convergence criterion is satisfied. In this article, it is considered that the pair (r, γ) , at a given point and in two subsequent time instants, reaches a prescribed tolerance.

In order to analyse post-delamination behaviour, a generic point j , which is the outer non-delaminated point, is considered (Fig. 2). The relative displacement of the points between point j and the free edge must be evaluated by an alternative procedure. It is conceived that the relative displacement r is calculated by spatial numerical integration of the strain. With this assumption, the displacements after delamination are calculated as follows:

$$u^u = \int_{x_j}^{x_{j+m}} \epsilon_{11}^u dx \quad (25a)$$

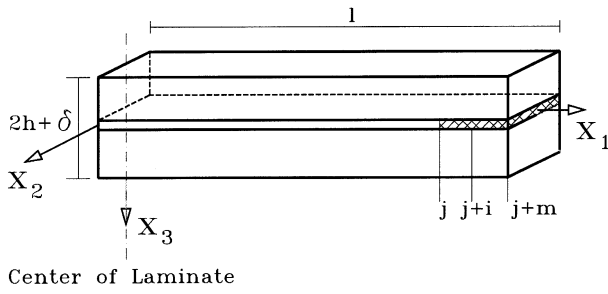


Fig. 2 Laminate showing a delaminated region

$$v^u = 2 \int_{x_j}^{x_{j+m}} \epsilon_{12}^u dx \tag{25b}$$

$$u^l = \int_{x_j}^{x_{j+m}} \epsilon_{11}^l dx \tag{25c}$$

$$v^l = 2 \int_{x_j}^{x_{j+m}} \epsilon_{12}^l dx \tag{25d}$$

which permits the relative displacements

$$\Delta u = u^u - u^l \tag{26a}$$

$$\Delta v = v^u - v^l \tag{26b}$$

to be obtained. Hence, the relative displacement of a generic point on the delaminated region is given by

$$r_{j+i} = r_j + (\sqrt{\Delta u^2 + \Delta v^2})_j^{j+i} \tag{27}$$

This is a simplified procedure, which represents a first approach to the problem. It should be pointed out that a more detailed analysis of this problem, involving the coupling between the interlaminar stresses and damage, which is beyond the scope of this contribution, must be carried out to validate it.

5 LAMINATED TUBE

As an application of the proposed model, an antisymmetric two-layer angle ply laminated tube, depicted in Fig. 3, is considered. The analysis is restricted to situations where lamina response occurs on elastic domain and where the composite failure occurs by delamination. With this assumption, either lamina or interface rupture cannot occur. This hypothesis is validated by the von Mises criterion for the interlayer and the Tsai–Hill criterion for the laminae [3].

Using the same assumptions employed by Bai *et al.* [15], i.e. each lamina has the same geometrical and material properties, equations (9) to (11) are simplified resulting in the ordinary differential equations

$$\frac{\delta}{G} \frac{d^2(\Delta\sigma_{11})}{dx_1^2} h = A_{1112}\sigma_{12} + B_{1111} \Delta\sigma_{11} + B_{1122} \Delta\sigma_{22} \tag{28}$$

$$0 = A_{2212}\sigma_{12} + B_{2211} \Delta\sigma_{11} + B_{2222} \Delta\sigma_{22} \tag{29}$$

$$\frac{\delta}{2G} \frac{d^2(\Delta\sigma_{12})}{dx_1^2} h = A_{1211}\sigma_{11} + B_{1222}\sigma_{22} + B_{1212} \Delta\sigma_{12} \tag{30}$$

with the following boundary conditions:

$$\Delta\sigma_{11}(-l) = \Delta\sigma_{11}(l) = 0 \tag{31a}$$

$$\Delta\sigma_{12}(-l) = \Delta\sigma_{12}(l) = 0 \tag{31b}$$

Solving this system, the constraint stresses are obtained:

$$\Delta\sigma_{11} = \frac{K_1}{D_1^2} \left(\frac{e^{D_1 x_1} + e^{-D_1 x_1}}{e^{D_1 l} + e^{-D_1 l}} - 1 \right) \tag{32a}$$

$$\Delta\sigma_{22} = -\frac{1}{B_{2222}} (B_{2211} \Delta\sigma_{11} - A_{2212} \sigma_{12}) \tag{32b}$$

$$\Delta\sigma_{12} = \frac{K_2}{D_2^2} \left(\frac{e^{D_2 x_1} + e^{-D_2 x_1}}{e^{D_2 l} + e^{-D_2 l}} - 1 \right) \tag{32c}$$

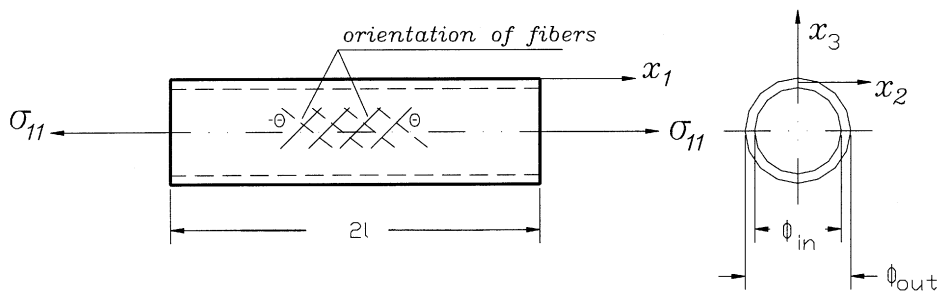


Fig. 3 Antisymmetric laminated tube [+theta, -theta]

where

$$K_1 = \frac{G}{\delta h} \left(A_{1112} - \frac{B_{1122}A_{2212}}{B_{2222}} \right) \sigma_{12} \quad (33a)$$

$$K_2 = \frac{2G}{\delta h} (A_{1211}\sigma_{11} + A_{1222}\sigma_{22}) \quad (33b)$$

$$D_1 = \sqrt{\frac{G}{\delta h} \left(B_{1111} - \frac{B_{1122}B_{2211}}{B_{2222}} \right)} \quad (33c)$$

$$D_2 = \sqrt{\frac{2GB_{1212}}{\delta h}} \quad (33d)$$

Therefore, the relations for the interlaminar stresses are given by

$$\tau_{13} = \frac{1}{2}C_1D_1(e^{D_1x_1} - e^{-D_1x_1})h \quad (34a)$$

$$\tau_{23} = \frac{1}{2}C_2D_2(e^{D_2x_1} - e^{-D_2x_1})h \quad (34b)$$

where

$$C_1 = \frac{A_{1112} - B_{1122}A_{2212}/B_{2222}}{\pi h D_1^2 (e^{-D_1l} + e^{D_1l})} \sigma_{12} \quad (35a)$$

$$C_2 = \frac{2(A_{1211}\sigma_{11} + A_{1222}\sigma_{22})}{\pi h D_2^2 (e^{-D_2l} + e^{D_2l})} \quad (35b)$$

As a first example, a $[+30^\circ/-30^\circ]$ laminated tube 60 mm long with 15 mm internal diameter and 2 mm thickness is considered. The composite AS/3501, whose properties are presented in Table 1, is constructed [2]. The constitutive properties of the interlayer are presented in Table 2 and their physical meaning is discussed in the analysis of the numerical simulations. A cyclic tensile stress load, depicted in Fig. 4, is also applied.

An analysis of state variables and thermodynamic forces is now in order. Time evolution of the relative displacement r is presented in Fig. 5a. After the delamination process is completed, the laminae are debonded, and there is a great

Table 1 Material properties

Material	E_1 (GPa)	E_2 (GPa)	G_{12} (GPa)	ν_{12}
AS/3501	138.0	9.0	6.9	0.30
Scotchply 1002	38.6	8.2	4.1	0.26

Table 2 Interface constitutive properties

k ($\times 10^9$ N/m ³)	a ($\times 10^9$ N/m ³)	b (m ² /J s ²)	c (m ³ /N s ²)	δ/G (m/Pa)
500	7	100	5×10^{-12}	10^{-13}

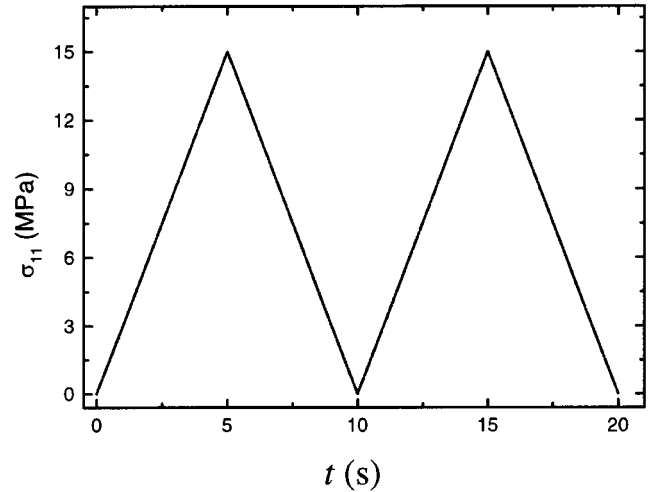


Fig. 4 Cyclic tensile stress load

relative displacement increase. This is a consequence of contact loss between the laminae that causes a loss of resistance. The thermodynamic force X^R is associated with the relative displacement and represents the contact stress between lamina and interlayer [9]. As can be seen in Fig. 5b, this variable has a maximum value before delamination begins to occur and, after this, decreases. It means a loss of resistive stress. When the laminae are debonded, there are small values of X^R , meaning that some contact stress remains to be provided by the adhesive [9, 10].

Damage variable evolution is presented in Fig. 5c and permits delamination evolution to be visualized. When $\gamma = 1$, delamination is completed and the laminae debonds. It is clear that the delamination process starts at the free edge and propagates to interior points. This result is in close agreement with experimental analysis [16] and is a consequence of asymptotic growth of interlaminar shear stresses in the free-edge region [26]. The thermodynamic force Y is associated with the damage variable γ and represents the energy necessary to promote the delamination process. As Fig. 5d shows, the maximum value of this variable is at the free edge meaning the high energy associated with delamination of this point. After delamination of the free edge, the Y value tends to decrease at other points. Observing the time evolution of Y at some particular point, this variable presents a maximum value and then decreases as delamination takes place. When the laminae are debonded, Y assumes null values.

Now, the influence of fibre angles on the delamination process is analysed by considering the same laminated tube of the preceding example and different fibre orientations: $[0^\circ/0^\circ]$, $[+45^\circ/-45^\circ]$ and $[+60^\circ/-60^\circ]$. The symmetric configuration $[0^\circ/0^\circ]$ presents no delamination since the absence of stiffness mismatch causes no interlaminar stresses. The other configurations present similar qualitative behaviours; however, a quantitative analysis presents some differences. The variable r has greater values for the

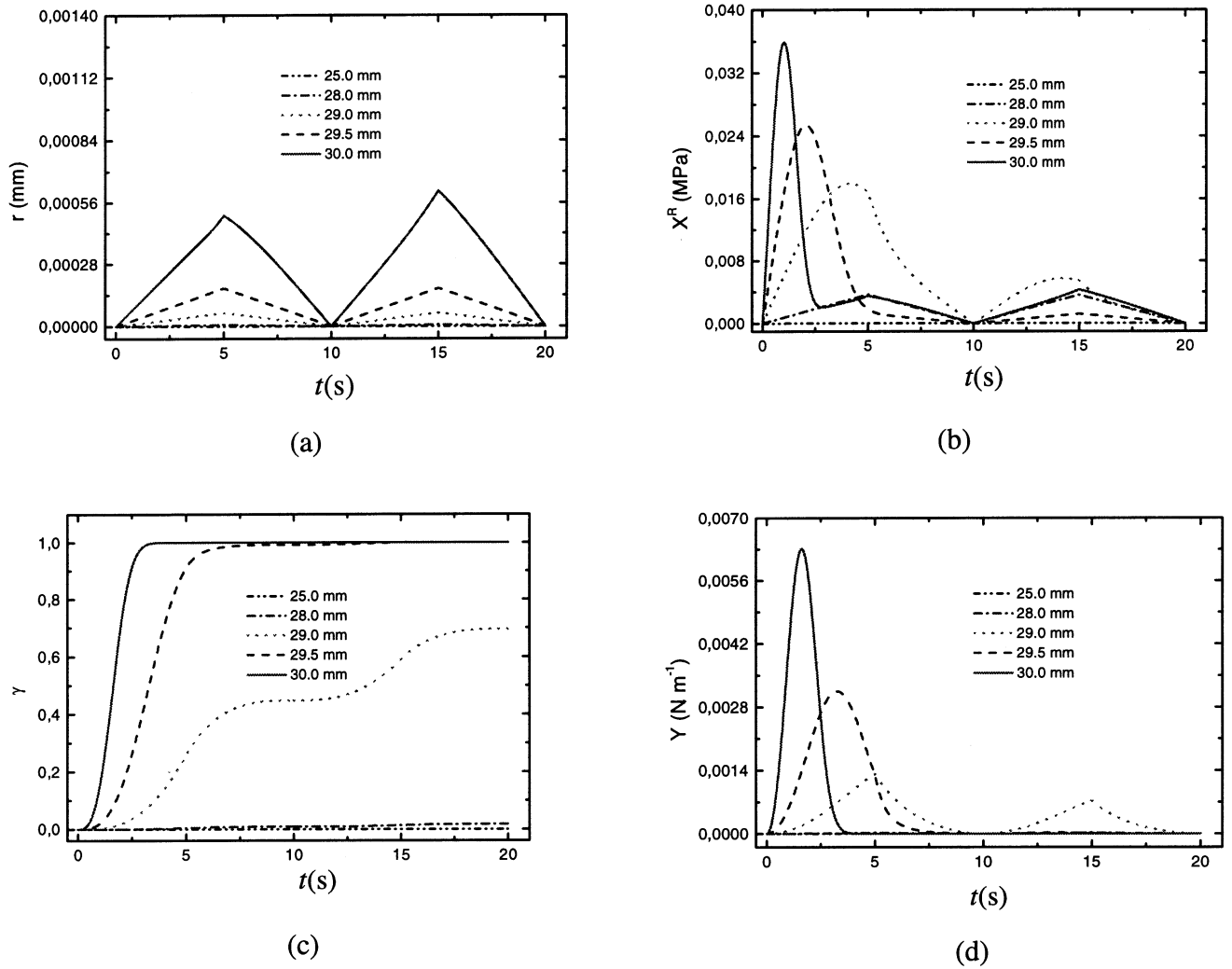


Fig. 5 Time evolution of the state variables and thermodynamic forces for a $[+30^\circ / -30^\circ]$ AS/3501 laminated tube, subjected to a cyclic tensile stress: (a) r ; (b) X^R ; (c) γ ; (d) Y

laminate $[+45^\circ / -45^\circ]$ and smaller values for $[+30^\circ / -30^\circ]$, while the laminate $[+60^\circ / -60^\circ]$ present medium values (Fig. 6). As a consequence, the damage process begins to take place earlier in the laminate $[+45^\circ / -45^\circ]$ (Fig. 7).

The preceding analysis confirms that the evolution of these variables is associated with the mechanical properties of the laminae. As expected, the delamination process is associated with the stiffness mismatch of adjacent laminae and, therefore, the fibre angle variation may become critical. Another example, which shows this, considers a comparison between two different laminates $[+45^\circ / -45^\circ]$. The first is a graphite–epoxy composite, AS/3501, while the second is a glass–fibre composite, Scotchply 1002, the properties of which are presented in Table 1. Since these materials present different kinds of anisotropy, distinct responses may be expected. The AS/3501 composite, where $E_1/E_2 \approx 15$, delaminates faster

than Scotchply 1002 composite where $E_1/E_2 \approx 5$ (Figs 8 and 9).

The influence of interface constants is now in order by considering a Scotchply 1002 composite. The rate δ/G is associated with the stress growth near the free edge. Figure 10 presents the evolution of damage variables γ for two different values of this relation ($\delta/G = 4.5 \times 10^{-13}$ and $\delta/G = 10^{-13}$). It must be noted that the reduction in δ/G causes a more effective delamination. On the other hand, Fig. 11 considers $a = 0$. In this simulation, it should be pointed out that the variable X^R assumes null values after the debonding of the laminae, meaning that there is no resistive contact between them, which contrasts with the previous results.

Next a shear stress load with the same characteristics of the normal stress presented in Fig. 4 is considered. This load process causes a significantly greater relative displacement r , changing the characteristics of the response. This

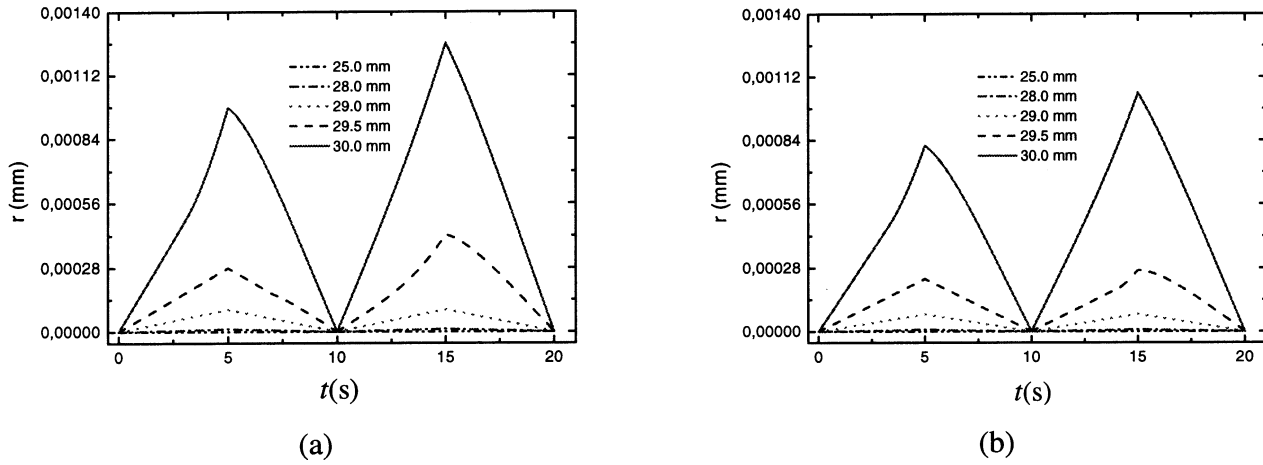


Fig. 6 Time evolution of the relative displacement variable r for an AS/3501 laminated tube, subjected to a cyclic tensile stress: (a) $[+45^\circ / - 45^\circ]$; (b) $[+60^\circ / - 60^\circ]$

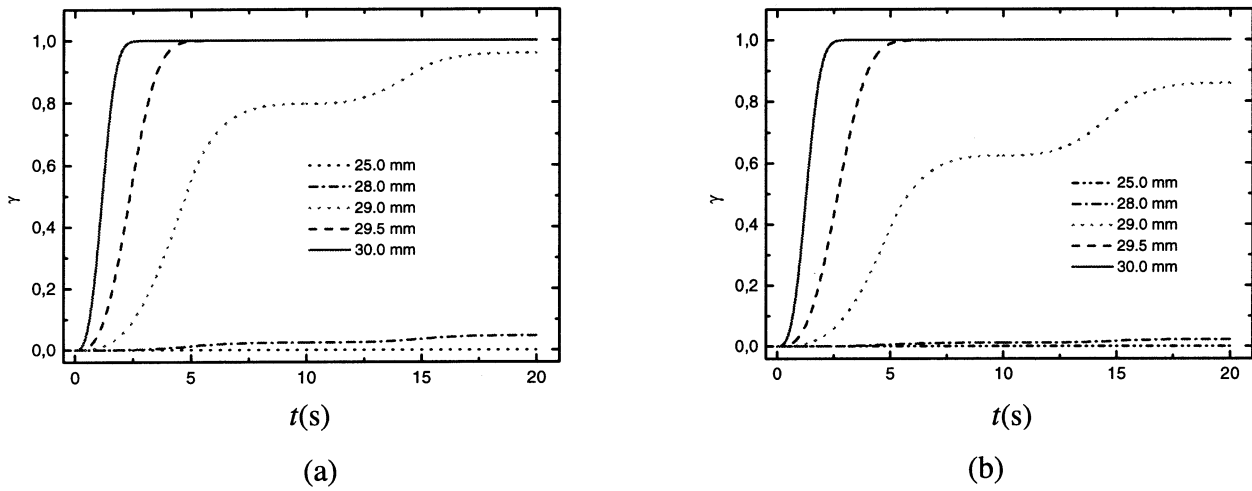


Fig. 7 Time evolution of the damage variable γ for an AS/3501 laminated tube, subjected to a cyclic tensile stress: (a) $[+45^\circ / - 45^\circ]$; (b) $[+60^\circ / - 60^\circ]$

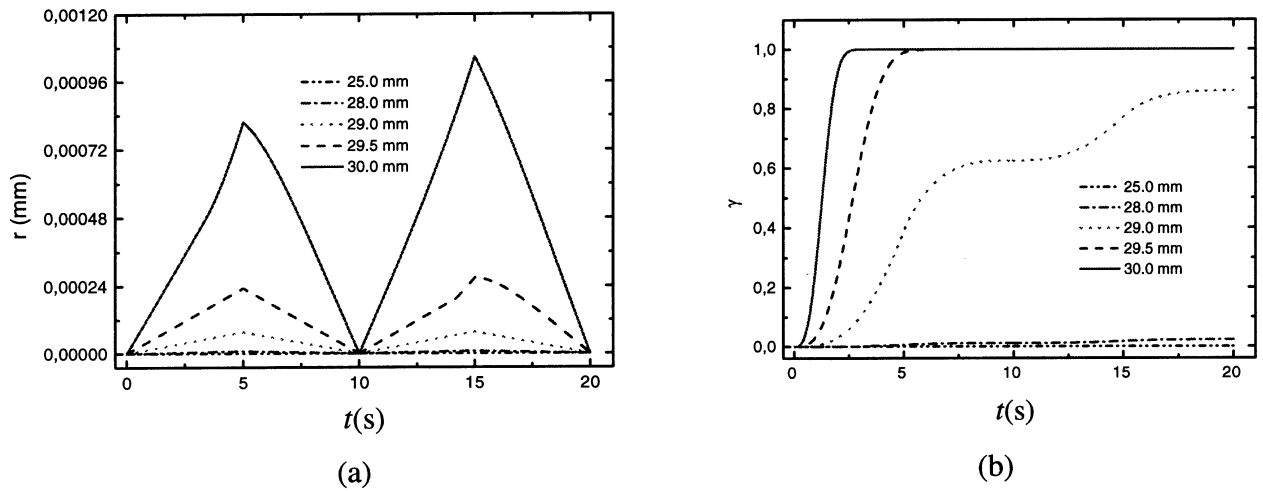


Fig. 8 Time evolution of the state variables for a $[+45^\circ / - 45^\circ]$ AS/3501 laminated tube, subjected to a cyclic tensile stress: (a) r ; (b) γ

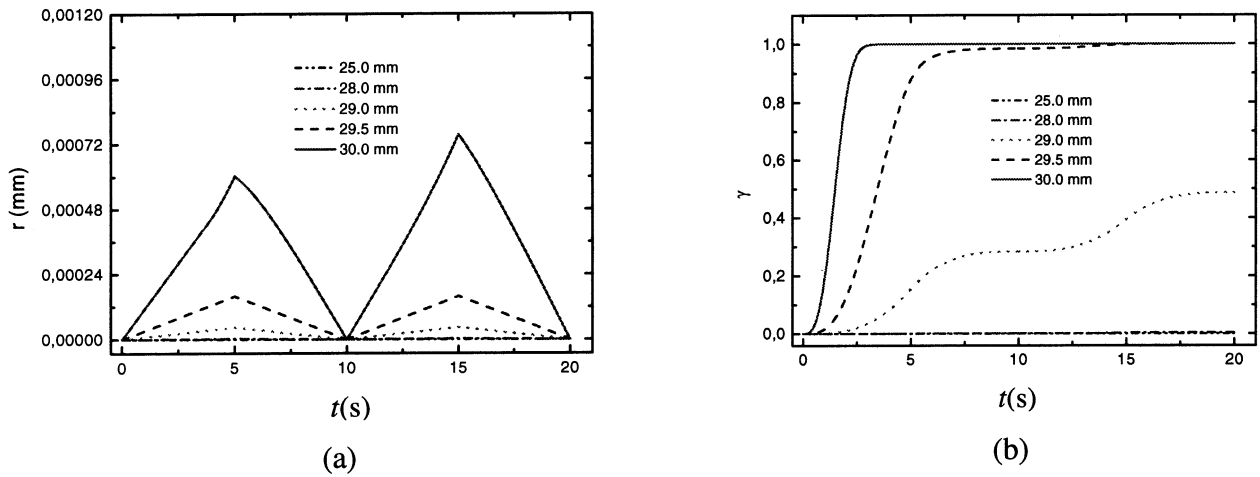


Fig. 9 Time evolution of the state variables for a [+45°/ - 45°] Scotchply 1002 laminated tube, subjected to a cyclic tensile stress: (a) r ; (b) γ

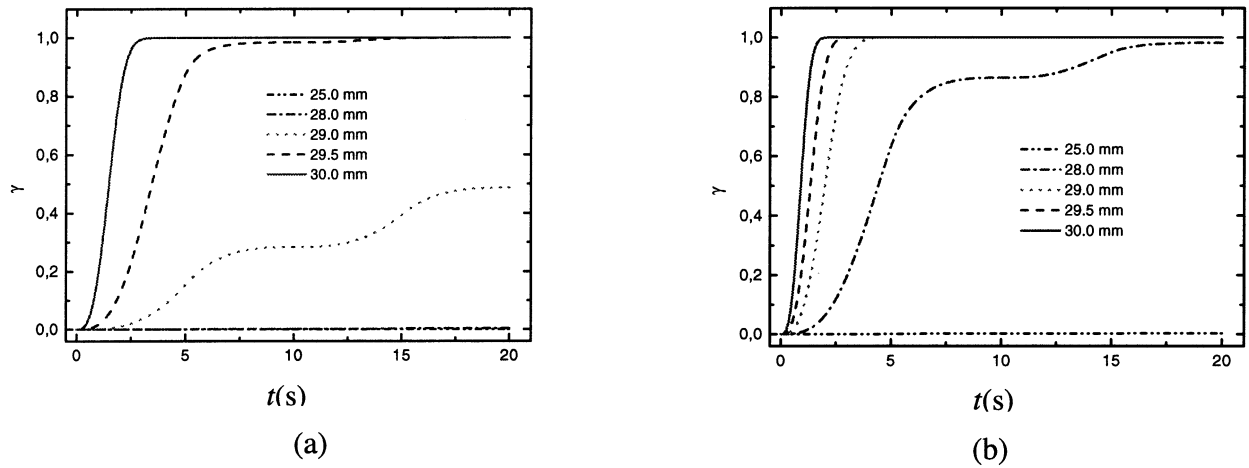


Fig. 10 Time evolution of the damage variable γ for a [+45°/ - 45°] Scotchply 1002 laminated tube, subjected to a cyclic tensile stress: (a) $\delta/G = 4.5 \times 10^{-13}$; (b) $\delta/G = 10^{-13}$

result is in agreement with physical considerations, which establish that the shear effect is critical to the delamination process (Fig. 12).

6 LAMINATED BAR

In order to consider another application of the proposed model, a two-layer angle ply laminated bar, depicted in Fig. 13, is considered. Once again, the analysis is restricted to situations where lamina response occurs in the elastic domain and where the composite failure occurs by delamination [3].

As an example, a laminated bar $2l$ long with a finite thickness interlayer δ and unitary depth, subjected to a tensile load, is considered. With this assumption, equations

(9) to (11) are simplified resulting in the following differential equation:

$$\frac{d^2(\Delta\sigma_{11})}{dx_1^2} - (D_1^v)^2 \Delta\sigma_{11} = K_1^v \tag{36}$$

where

$$D_1^v = \sqrt{\frac{G}{\delta h} B_{1111}} \tag{37a}$$

$$K_1^v = \frac{G}{\delta h} A_{1111} \sigma_{11} \tag{37b}$$

Establishing the equilibrium of the upper lamina, the following relation between interlaminar stress and the constraint stress $\Delta\sigma_{11}$ is obtained:

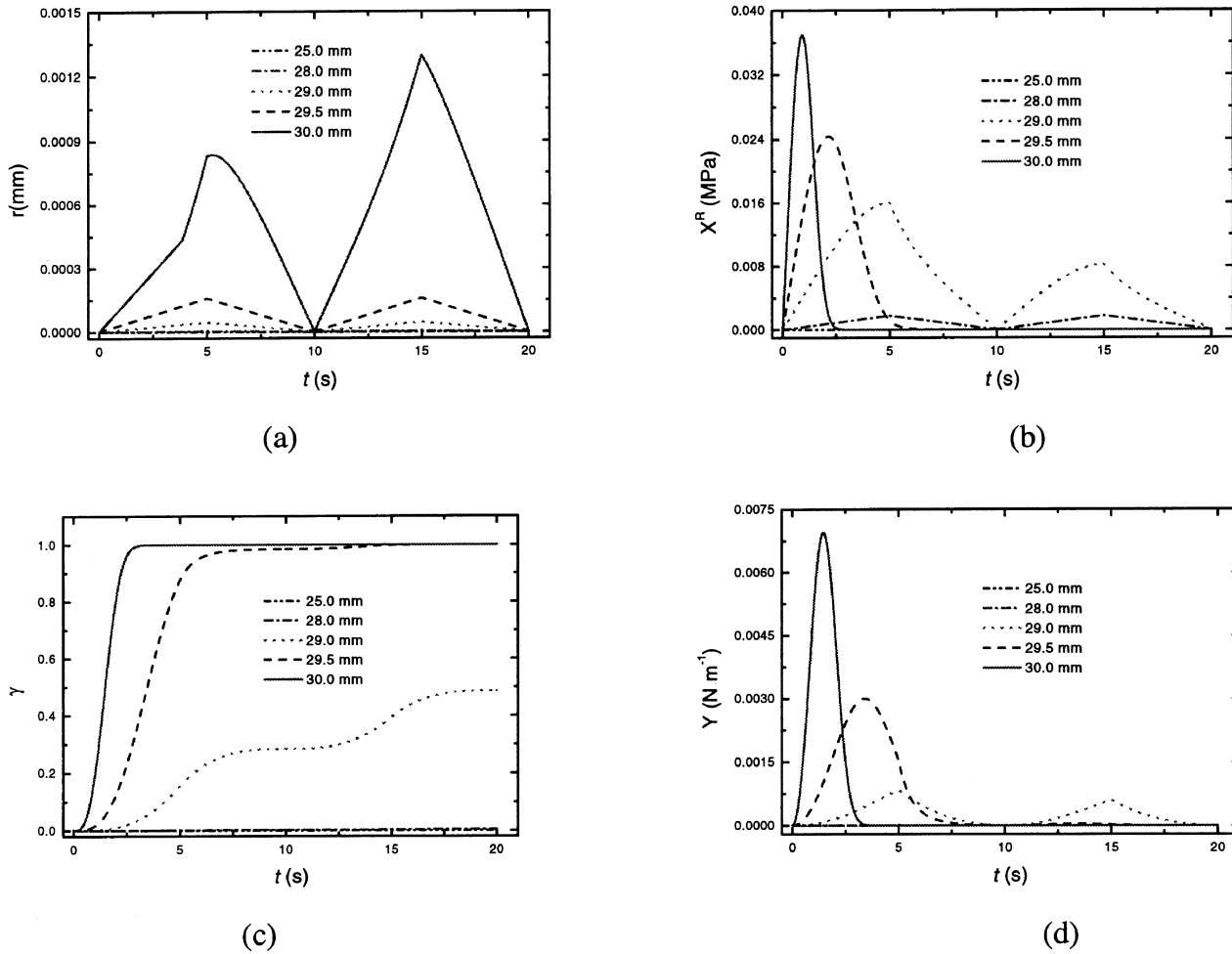


Fig. 11 Time evolution of the state variables and thermodynamic forces for a $[+45^\circ/-45^\circ]$ Scotchply 1002 laminated tube, subjected to a cyclic tensile stress with $a = 0$: (a) r ; (b) X^R ; (c) γ ; (d) Y

$$\tau_{13} = \frac{h}{2} \frac{d(\Delta\sigma_{11})}{dx_l} \tag{38}$$

Applying the boundary conditions, $\Delta\sigma_{11}(l) = \Delta\sigma_{11}(-l) = 0$, the solution of equation (36) is given by

$$\Delta\sigma_{11} = \frac{K_1^v}{(D_1^v)^2} \frac{(e^{x_1 D_1^v} + e^{-x_1 D_1^v})}{(e^{x_1 l} + e^{-x_1 l})} - \frac{K_1^v}{(D_1^v)^2} \tag{39}$$

Using equation (38), the interlaminar stress is

$$\tau_{13} = \frac{h K_1^v}{2 D_1^v} \frac{(e^{x_1 D_1^v} - e^{-x_1 D_1^v})}{(e^{x_1 l} + e^{-x_1 l})} \tag{40}$$

Now, it is possible to evaluate the relative displacement Δu from the linear shear theory [22]:

$$\Delta u = \frac{\delta}{G} \tau_{13} \tag{41}$$

To illustrate the bar response, a $[0^\circ/90^\circ]$ laminated bar

60 mm long where each lamina has a thickness $h = 1$ mm is considered. The material is AS/3501 composite whose properties are presented in Table 1 and the constitutive properties of the interlayer are presented in Table 2. A cyclic tensile stress load, depicted in Fig. 4, is also applied.

An analysis of state variables and thermodynamic forces is now in order. As expected, this behaviour is qualitatively similar to the laminated tube response and the physical interpretation of state variables and thermodynamic forces are the same (Fig. 14).

Next, a different loading process is considered (Fig. 15). For this situation, delamination occurs in a pronounced form as a consequence of the high level of stress variation, which induces high interlaminar stresses. Figure 16 shows the time evolution of state variables and thermodynamic forces.

7 CONCLUSIONS

This contribution reports a model to describe delamination

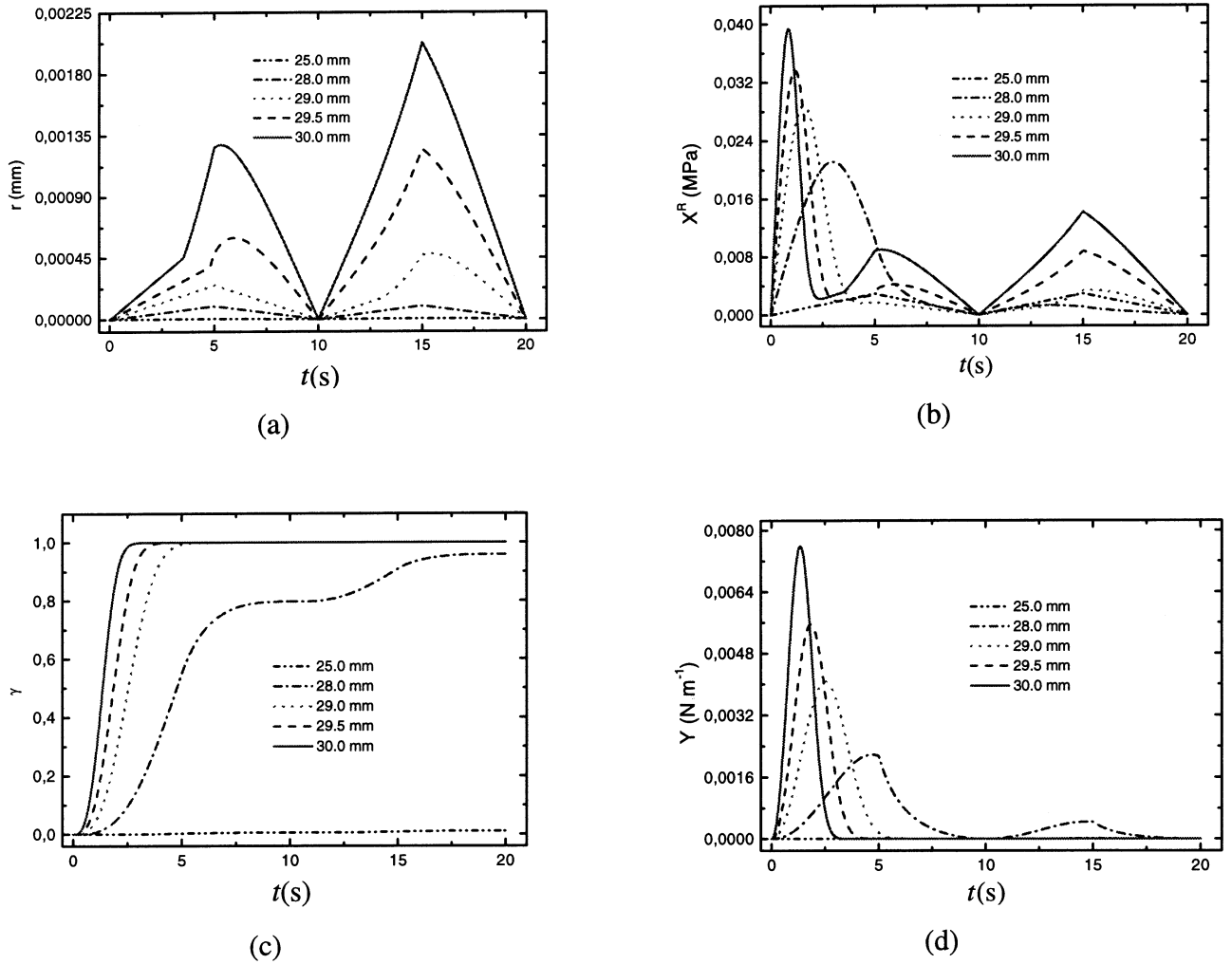


Fig. 12 Time evolution of the state variables and thermodynamic forces for a $[+45^\circ / -45^\circ]$ AS/3501 laminated tube, subjected to a cyclic tensile stress: (a) r ; (b) X^R ; (c) γ ; (d) Y

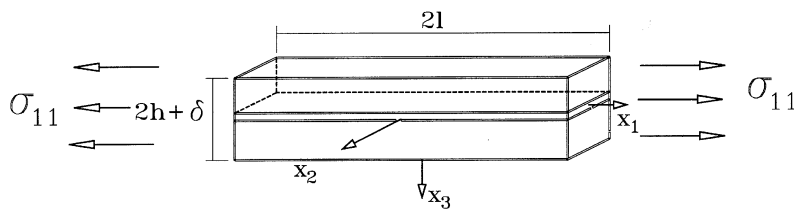


Fig. 13 Laminated bar $[+\theta, -\theta]$

in laminated composite materials. The proposed model considers a laminate with a finite thickness interlayer. Interlaminar stresses are evaluated from a modified lamination theory. This result is used as input in a constitutive adhesion model that describes the damage evolution of the interlayer. An iterative numerical procedure is developed, solving the model equations separately. Numerical simulations of a laminated tube and a laminated bar are considered as applications of the proposed general formulation. An analysis of state variables and thermodynamic forces is

presented, explaining their physical meaning. Numerical results show that the model is capable of capturing the general behaviour of the experimental data available in literature. Some improvements to the model are still needed, e.g. the consideration of different damage variables for each interface and also the intralaminar damage. Further, it is important to validate the procedure employed to evaluate the relative displacement in the post-delamination response. Another improvement involves the calculation of the interlaminar stresses using some numerical

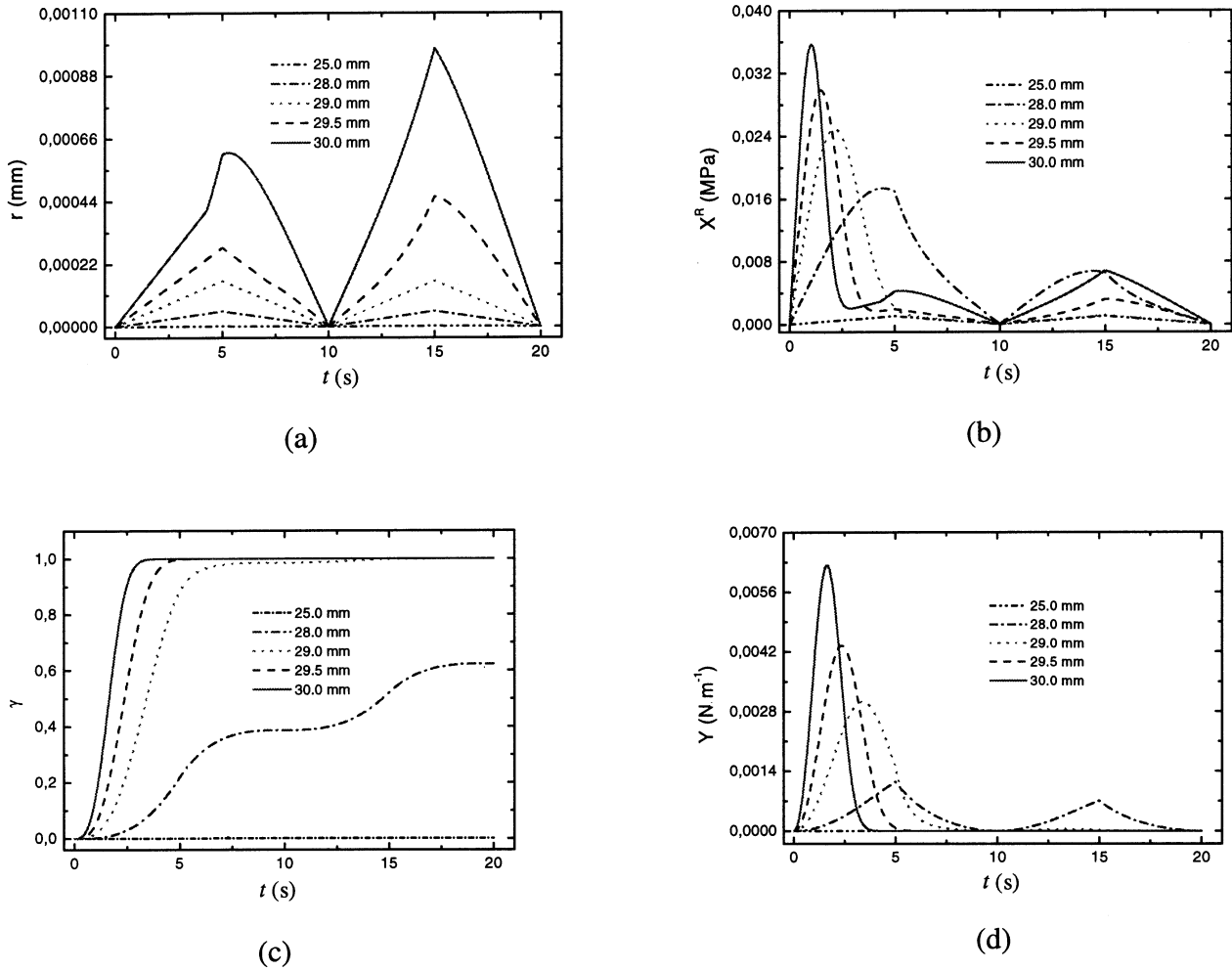


Fig. 14 Time evolution of the state variables and thermodynamic forces for a $[0^\circ/90^\circ]$ AS/3501 laminated bar, subjected to a cyclic tensile stress: (a) r ; (b) X^R ; (c) γ ; (d) Y

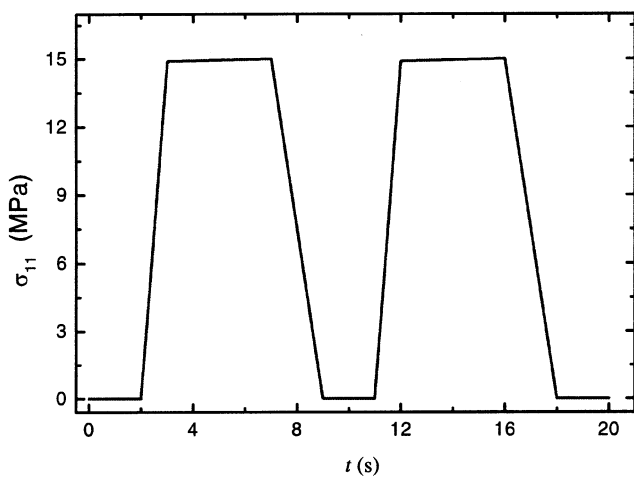


Fig. 15 Cyclic tensile stress load

procedure, such as the finite element method. This will permit analysis of other laminated structures, taking into account different kinds of effect and amplifying the scope of application of the proposed model. Finally, experimental analysis is necessary for quantitative validation of the proposed model and for an accurate determination of the properties of the interlayer.

ACKNOWLEDGEMENT

The authors acknowledge the support of the CNPq Conselho Nacional de Desenvolvimento Científico e Tecnológico, Brazil.

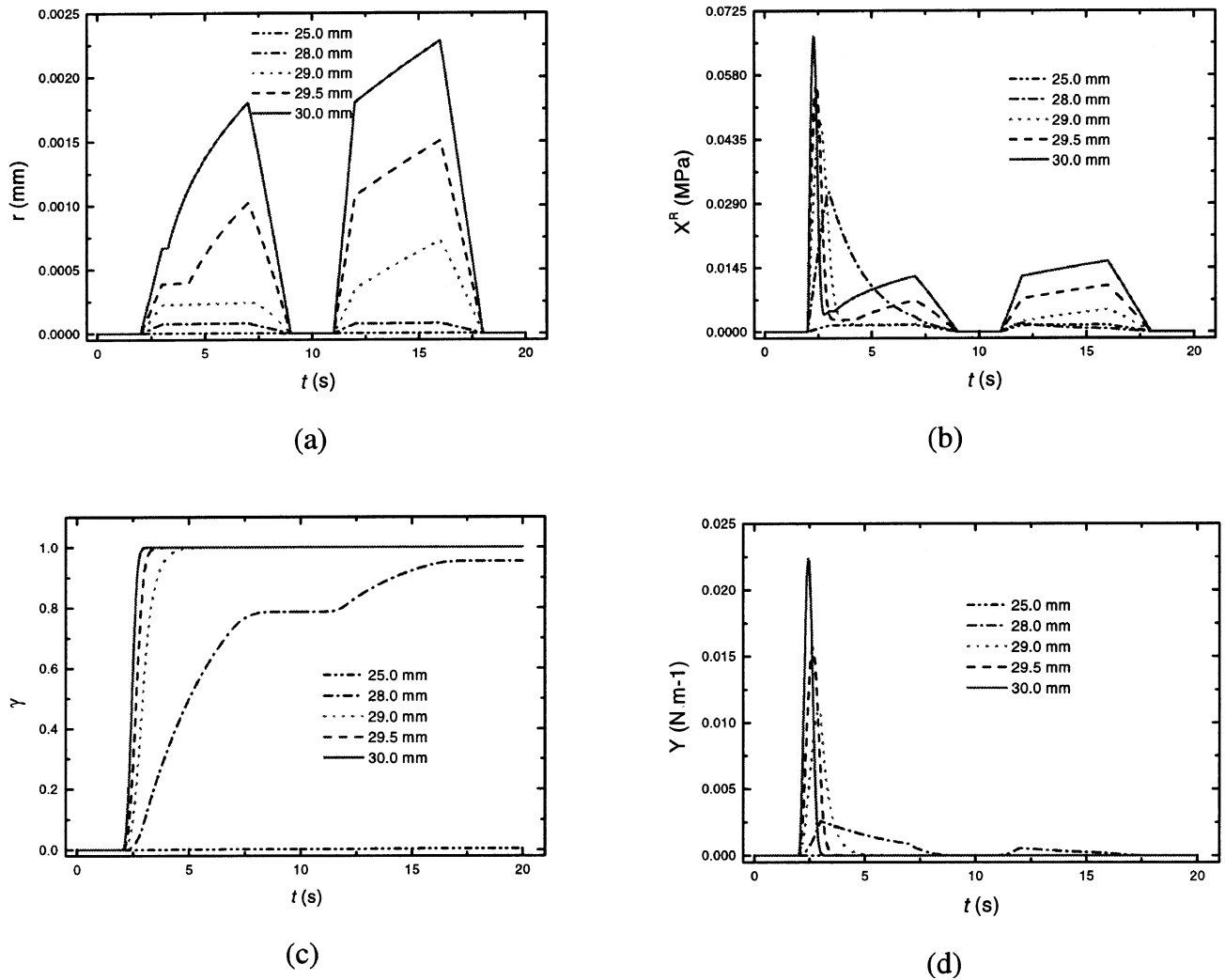


Fig. 16 Time evolution of the state variables and thermodynamic forces for a [0°/90°] AS/3501 laminated bar, subjected to a cyclic tensile stress: (a) r ; (b) X^R ; (c) γ ; (d) Y

REFERENCES

- 1 Point, N. and Sacco, E. A delamination model for laminated composites. *J. Solids and Structs*, 1996, **33**(4), 483–509.
- 2 Reddy, J. N. *Mechanics of Laminated Composite Plates—Theory and Analysis*, 1997 (CRC Press, Boca Raton, Florida).
- 3 Gibson, R. F. *Principles of Composite Materials Mechanics*, 1994 (McGraw-Hill, New York).
- 4 O’Brien, T. K. Characterization of delamination onset and growth in a composite laminate. In *Damage in Composite Materials* (Ed. K. L. Reifsnider), ASTM STP 775, 1982 (American Society for Testing and Materials, Philadelphia, Pennsylvania).
- 5 O’Brien, T. K. Analysis of local delamination and their influence on composite laminate behavior. In *Delamination and Debonding of Materials* (Ed. W. S. Johnson), ASTM STP 887, 1985 (American Society for Testing and Materials, Philadelphia, Pennsylvania).
- 6 Ousset, Y. Numerical simulation of delamination growth in layered composite plates. *Eur. J. Mechanics A—Solids*, 1999, **18**(2), 291–312.

- 7 Yin, W. L. Delamination: laminate analysis and fracture mechanics. *Fatigue Fracture Engng Mater. Structs*, 1998, **21**(4), 509–520.
- 8 Point, N. and Sacco, E. Mathematical properties of a delamination model. *Math. Computer Modelling*, 1998, **28**(4–8), 359–371.
- 9 Fremond, M., Sacco, E., Point, N. and Tien, J. M. T. D. Contact with adhesion. In Proceedings of the 1996 ASME Engineering Systems Design and Analysis Conference, 1996, PD-Vol. 76, pp.151–156 (American Society of Mechanical Engineers, New York).
- 10 Tien, J. M. T. D. Contact avec adhérence. Thèse de Doctorat d’Etat Es-Sciences Mathématiques, L’Université Paris VI, 1990.
- 11 Point, N. Approche mathématique de problèmes à frontières libres: application à des exemples physiques. Thèse de Doctorat d’Etat Es-Sciences Mathématiques, L’Université Paris XIII, 1989.
- 12 Fremond, M. Contact unilatéral avec adhérence. In *Unilateral Problems in Structural Analysis* (Eds G. Del Piero and F. Maceri), 1985 (Springer-Verlag, Berlin).

- 13 **Fremond, M.** Adhérence des solides. *J. Méc. Théor. Appl.*, 1987, **6**, 383–407.
- 14 **Fremond, M.** Contact with Adhesion. In *Topics in Nonsmooth Mechanics* (Eds J. J. Moureau, P. D. Panagiotopoulos and G. Strang), 1988 (Birkhäuser, Basel).
- 15 **Bai, Q. S., Murakami, S. and Kanagawa, Y.** A lamination theory incorporating the effect of interlaminar deformation. *J. Composite Mater.*, 1997, **31**(20), 2052–2073.
- 16 **Pipes, R. B. and Pagano, N. J.** Interlaminar stresses in composite laminates under uniform axial extension. *J. Composite Mater.*, 1970, **4**, 538–548.
- 17 **Mackerle, J.** Delamination of composites—finite element and boundary element analysis—a bibliography (1995–1997). *Finite Elements Analysis Des.*, 1998, **30**(3), 243–252.
- 18 **Pradhan, S. C. and Tay, T. E.** Three-dimensional finite element modelling of delamination growth in notched composite laminates under compression loading. *Engng Fracture Mechanics*, 1998, **60**(2), 157–171.
- 19 **Mi, Y., Crisfield, M. A., Davies, G. A. O. and Hellweg, H. B.** Progressive delamination using interface elements. *J. Composite Mater.*, 1998, **32**(14), 1246–1272.
- 20 **Marchuk, A. V.** Finite element construction for simulating delamination of sandwich composite plates and masses. *Mechanics Composite Mater.*, 1998, **34**(2), 184–193.
- 21 **Roche, C. H. and Accorsi, M. L.** A new finite element for global modeling of delaminations in laminated beams. *Finite Elements Analysis Des.*, 1998, **31**(2), 165–177.
- 22 **Lu, X. and Liu, D.** Interlayer shear slip theory for cross-ply laminates with nonrigid interfaces. *Am. Inst. Aeronaut. Astronaut. J.*, 1992, **30**(4), 1063–1073.
- 23 **Lemaitre, J. and Chaboche, J. L.** *Mechanics of Solid Materials*, 1990 (Cambridge University Press, Cambridge).
- 24 **Rockafellar, R. T.** *Convex Analysis*, 1970 (Princeton Press, Princeton, New Jersey).
- 25 **Eringen, A. C.** *Mechanics of Continua*, 1967 (John Wiley, New York).
- 26 **Wang, S. S. and Choi, I.** Boundary-layer effects in composite laminates. Part II: free-edge stress solutions and basic characteristics. *J. Appl. Mechanics*, 1982, **49**, 549–560.